Strahlenther Onkol (2018) 194:719–726
https://doi.org/10.1007/s00066-018-1292-4

ORIGINAL ARTICLE

Voxel-wise correlation of functional imaging parameters in HNSCC patients receiving PET/MRI in an irradiation setup

Kerstin Zwirner[1] · Daniela Thorwarth[2,3] · René M. Winter[2] · Stefan Welz[1,3] · Jakob Weiss[4] · Nina F. Schwenzer[4] · Holger Schmidt[4] · Christian la Fougère[3,5] · Konstantin Nikolaou[3,4] · Daniel Zips[1,3] · Sergios Gatidis[4]

Received: 20 November 2017 / Accepted: 5 March 2018 / Published online: 21 March 2018

Abstract

Purpose The purpose of this study was to demonstrate the feasibility of voxel-wise multiparametric characterization of head and neck squamous cell carcinomas (HNSCC) using hybrid multiparametric magnetic resonance imaging and positron emission tomography with [^{18}F]-fluorodesoxyglucose (FDG-PET/MRI) in a radiation treatment planning setup.

Methods Ten patients with locally advanced HNSCC were examined with a combined FDG-PET/MRI in an irradiation planning setup. The multiparametric imaging protocol consisted of FDG-PET, T2-weighted transverse short tau inversion recovery sequence (STIR) and diffusion-weighted MRI (DWI). Primary tumours were manually segmented and quantitative imaging parameters were extracted. PET standardized uptake values (SUV) and DWI apparent diffusion coefficients (ADC) were correlated on a voxel-wise level.

Results Images acquired in this specialised radiotherapy planning setup achieved good diagnostic quality. Median tumour volume was 4.9 [1.1–42.1] ml. Mean PET SUV and ADC of the primary tumours were 5 ± 2.5 and 1.2 ± 0.3 10^{-3} mm^2/s, respectively. In voxel-wise correlation between ADC values and corresponding FDG SUV of the tumours, a significant negative correlation was observed ($r = -0.31 \pm 0.27$, $p < 0.05$).

Conclusion Multiparametric voxel-wise characterization of HNSCC is feasible using combined PET/MRI in a radiation planning setup. This technique may provide novel insights into tumour biology with regard to radiation therapy in the future.

Keywords Magnetic Resonance Imaging · Multimodal Imaging · Positron-Emission Tomography · Radiotherapy · Head and Neck Neoplasms

Clinical trial registration number: NCT-02666885.

✉ Kerstin Zwirner, M.D.
Kerstin.Zwirner@med.uni-tuebingen.de

[1] Department of Radiation Oncology, Medical Faculty and University Hospital, Eberhard Karls University Tübingen, Hoppe-Seyler-Str. 3, 72076 Tübingen, Germany

[2] Section for Biomedical Physics, Department of Radiation Oncology, Medical Faculty and University Hospital, Eberhard Karls University Tübingen, Hoppe-Seyler-Str. 3, 72076 Tübingen, Germany

[3] German Cancer Research Center (DKFZ) partner site Tübingen, German Cancer Consortium (DKTK), Hoppe-Seyler-Str. 3, 72076 Tübingen, Germany

[4] Department of Diagnostic and Interventional Radiology, Medical Faculty and University Hospital, Eberhard Karls University Tübingen, Hoppe-Seyler-Str. 3, 72076 Tübingen, Germany

[5] Division of Nuclear Medicine and Clinical Molecular Imaging, Department of Radiology, Medical Faculty and University Hospital, Eberhard Karls University Tübingen, Otfried-Müller-Straße 14, 72076 Tübingen, Germany

Voxelweise Korrelation funktioneller PET/MRT-Parameter in Bestrahlungslagerung bei Patienten mit Kopf-Hals-Tumoren

Zusammenfassung

Hintergrund Ziel der Studie war es, die Realisierbarkeit einer voxelweisen multiparametrischen Charakterisierung von Kopf-Hals-Tumoren mittels kombinierter Magnetresonanztomographie und Positronen-Emissions-Tomographie mit [^{18}F]-Fluordesoxyglukose (FDG-PET/MRT) in Bestrahlungsposition zu untersuchen.

Methoden Zehn Patienten mit lokal fortgeschrittenen Kopf-Hals-Tumoren wurden mittels FDG-PET/MRT in Bestrahlungslagerung untersucht. Das multiparametrische Bildgebungsprotokoll beinhaltete FDG-PET, eine transversale T2-gewichtete STIR-Sequenz („short tau inversion recovery“) sowie eine verzerrungsoptimierte Diffusionsbildgebung (DWI). Die Primärtumoren wurden zunächst manuell segmentiert. Anschließend wurden die quantitativen Bildgebungsparameter extrahiert. PET-SUV (standardized uptake values) und DWI-ADC (apparent diffusion coefficients) wurden voxelweise korreliert.

Ergebnisse Die Bildgebung, die in diesem speziellen radioonkologischen Setup erhoben wurde, erreichte gute diagnostische Qualität. Das mediane Tumorvolumen betrug 4,9 ml (Spanne 1,1–42,1 ml). Die jeweiligen durchschnittlichen PET-SUV- und ADC-Werte der Primärtumoren ergaben $5 \pm 2{,}5$ und $1{,}2 \pm 0{,}3\ 10^{-3}\,mm^2/s$. Die voxelweise Korrelation zwischen ADC-Werten und den dazugehörigen PET-SUVs der Tumoren zeigte eine signifikante negative Korrelation ($r = -0{,}31 \pm 0{,}27$; $p < 0{,}05$).

Schlussfolgerung Multiparametrische voxelweise Charakterisierungen von Kopf-Hals-Tumoren mittels kombiniertem PET/MRT sind in der Bestrahlungslagerung realisierbar. Diese Technik könnte zukünftig neuartige Einblicke in die Tumorbiologie im Hinblick auf die Strahlentherapie ermöglichen.

Schlagworte Magnetresonanztomographie · Multiparametrische Bildgebung · Positronen-Emissions-Tomographie · Strahlentherapie · Kopf-Hals Tumore

Introduction

Multiparametric imaging, hybrid imaging techniques and translation of acquired imaging information into a radiotherapeutic setup imply challenges and opportunities for improvement in precision medicine for cancer patients [1].

In patients with head and neck squamous cell carcinoma (HNSCC), magnetic resonance imaging (MRI) offers the advantage of high soft-tissue contrast of complex anatomy [2–4] and the option of additional functional imaging in vivo [5]. As a promising functional tool, MRI-based diffusion-weighted imaging (DWI) is related to motion of water molecules depending on the density, cell size and membrane characteristics of surrounding tissue microstructures, and is quantified by apparent diffusion coefficient (ADC) values [6]. Hereby, increased cellularity of malignant tumours in the head and neck region is usually reflected in decreased ADC measurements compared to normal tissue [7].

Positron-emission tomography with [^{18}F]-fluorodeoxyglucose (FDG-PET) has also been shown to be a sensitive imaging technique in HNSCC [8–10]. FDG-PET reflects the glucose consumption of the tumour and provides additional metabolic information that can be used for staging and treatment response. For quantification in malignant lesions, the standardized uptake value (SUV) is a widely used index for tumour glucose metabolism [11].

In this way, hybrid systems which integrate the advantages of MRI and positron-emission tomography (PET) into fused imaging techniques (PET/MRI) appear promising to improve diagnostics, describe molecular tumour biology and to investigate heterogeneity [5]. The complementary strengths of these two imaging techniques and the countercompensation for particular deficiencies (e.g. MRI compensates the inferior soft-tissue contrast of FDG-PET scans; FDG-PET supports more robust tumour detection in case of MRI artefacts) motivate increased implementation in clinical procedures [12].

The purpose of this study was to demonstrate the feasibility of voxel-wise multiparametric characterization of HNSCC using hybrid multiparametric FDG-PET/MRI in a radiotherapy (RT) treatment planning setup. Focusing on precision medicine, these data could be integrated into radiation treatment planning, dose painting and adaptive RT as additional molecular and functional information [13]. Therefore, as a proof of principle, the PET/MRI image acquisition was performed by a dedicated treatment planning hardware solution that has been described previously [14, 15].

The technical motivation of this feasibility study implied the evaluation of image quality, as the RT planning setup might potentially induce magnetic field inhomogeneity with special regard to the DWI sequences.

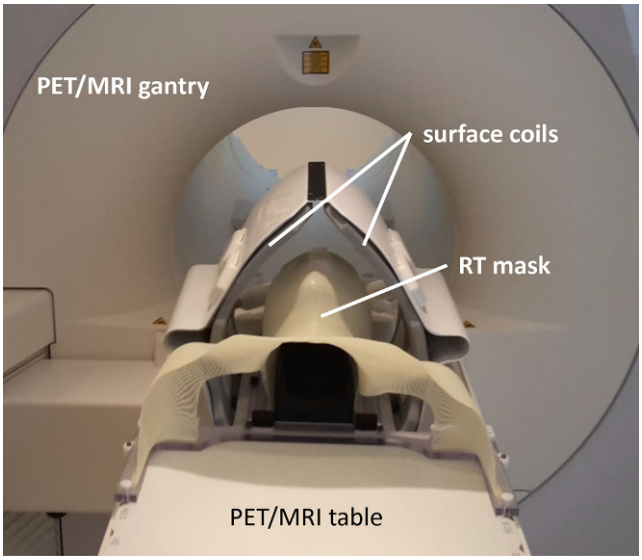

Fig. 1 Imaging setup using a preformed thermoplastic mask and a radiotherapy (*RT*) table overlay within the hybrid positron emission tomography/magnetic resonance imaging (PET/MRI) framework

Furthermore, the clinical motivation aims at subsequent implementation of functional imaging parameters in biologically adapted radiotherapy, e.g. in terms of defining a boost subvolume according to FDG uptake and/or diffusion-restricted areas. Most likely, several parameters should be considered to create an appropriate boost subvolume. Therefore, a hybrid multiparametric imaging technique seems relevant to reduce the level of registration uncertainty and to save scan time.

Materials and methods

Patient selection and setup

A cohort of ten male patients (49–71 years; mean 59 years) with histologically proven locally advanced HNSCC of the oro- or hypopharynx were included in this pilot investigation of a prospective study (NCT-02666885). The study was approved by the local ethics committee and all patients declared their written informed consent. All patients received computed tomography (CT) for staging before recruitment. Inclusion criterion was a pretherapeutic tumour board recommendation suggesting surgical resection with subsequent adjuvant radio(chemo)therapy.

Prior to surgical resection, all patients received FDG-PET/MRI of the head and neck in a specialised irradiation setup that has been published previously [14, 15]: patients were placed within the scanner lying on a radiotherapy planning board in supine position; the head was covered by a preformed thermoplastic mask, ensuring examination in RT position. Two 6-channel surface coils and two 6-channel spine coils were used for image acquisition, replacing the usual head and neck coils used in diagnostic setups without planning mask. In Fig. 1 an exemplary setup is shown.

Imaging

Imaging studies were performed on a clinical hybrid PET/MRI scanner capable of simultaneous acquisition of MRI and PET data (Biograph mMR, Siemens, Erlangen, Germany, 3 T). After i. v. injection of 235 ± 8 MBq [^{18}F]-FDG, patients were positioned according to the radiotherapy setup and FDG-PET data were acquired continuously during the entire scan time starting 30 min after tracer injection. The acquired time frame of 60–70 min post injection was reconstructed and used within this study. PET data were reconstructed using a three-dimensional ordered subset expectation maximization algorithm (OSEM) with the following parameters: iterations 3; subsets 21; matrix size 256 × 256; voxel size 2.8 × 2.8 × 2 mm; and Gaussian filter 3 mm. Attenuation correction (AC) was performed using the vendor-provided segmentation-based approach after acquisition of a dedicated T1-weighted dual echo gradient echo sequence for water/fat separation. In addition, an attenuation map of the radiation treatment planning setup was created via CT scan and incorporated as a CT-based AC template into the PET/MRI scanner's attenuation correction data base. This template was used for additional AC of the radiation treatment planning setup [15].

Amongst others, MRI sequences included a T2-weighted turbo spin echo sequence (transverse short tau inversion recovery sequence [STIR], resolution 0.7 × 0.7 mm^2, slice thickness 4 mm, repetition time 6130 ms, echo time 37 ms, inversion time 220 ms, flip angle 140°) and an echo-planar imaging-based DWI sequence (*b*-values of 150 and 800 s/mm^2, resolution 1.8 × 1.8 mm^2, slice thickness 5 mm, repetition time 4000 ms, echo time 64 ms, flip angle 180°, bandwidth 1736 Hz/Px, parallel imaging acceleration factor 2 using generalized autocalibrating partial parallel acquisition [GRAPPA], partial Fourier factor 7/8, spectral fat saturation) that were used for the present evaluation. A specialised method of distortion correction was applied as published by Winter et al. previously [15].

Data analysis

Image quality was assessed visually and by using an ordinal scoring system for the distortion-corrected diffusion-weighted sequence. To this end, the occurrence of image distortion, ghosting artefacts and residual fat signal was scored on a 4-point Likert scale (1 = no relevant artefacts, 4 = heavily corrupted image) by two experienced radiologists (W.J. and G.S.) in consensus.

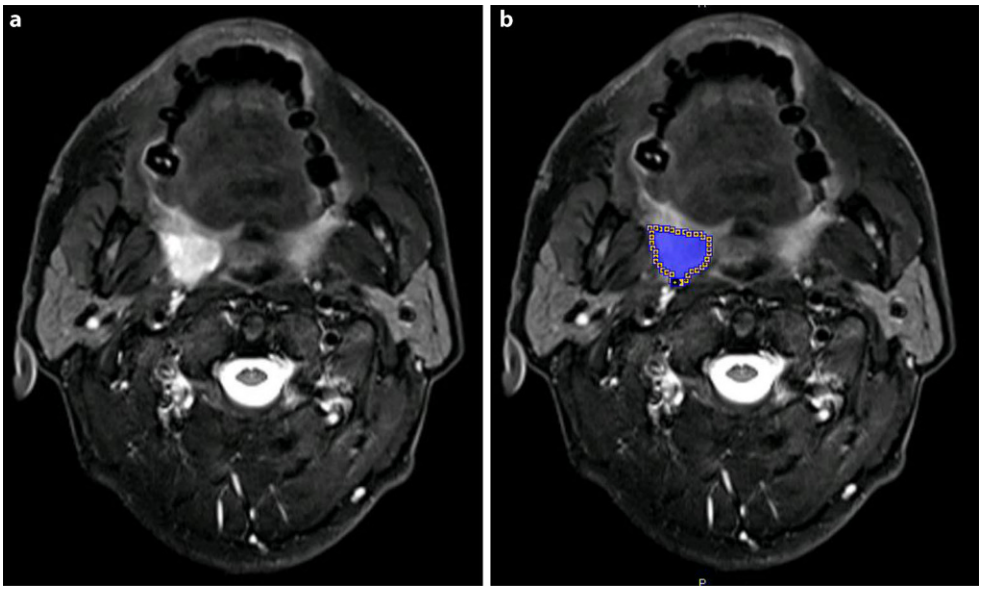

Fig. 2 Exemplary segmentation of the tumour (*blue area*)

Primary tumours were manually segmented on the T2-weighted transverse STIR sequence by a radiologist (6 years of experience) and a radiation oncologist in training (4 years of experience) in consensus using the software pmod (PMOD technologies, Zurich, Switzerland). An exemplary segmentation is shown in Fig. 2. Tumour volumes were quantified from the resulting segmentations.

For voxel-wise analysis, data sets of T2-weighted STIR, PET and DWI were resampled to the lowest resolution of these sequences in each dimension. Voxel values of PET and DWI were then extracted within the segmented tumour regions.

Numerical data are given as mean ± standard deviation or median and range where appropriate.

Correlation of voxel values of DWI and PET was assessed by calculating Spearman correlation coefficients using Matlab (The Mathworks, Natick, USA). *P*-values <0.05 were considered statistically significant.

Results

Patient, tumour and treatment characteristics are shown in Table 1. Surgery was performed in the range of 4–17 days after PET/MRI. All but one patient underwent surgery and received adjuvant radio(chemo)therapy. In one patient, due to reevaluation of tumour extent after PET/MRI, a definitive radiochemotherapy was performed.

Good diagnostic image quality was achieved in all patients using the radiotherapy planning setup described above. Visual rating of image artefacts on the DWI sequence according to a Likert scale showed moderate occurrence of ghosting and residual fat signal (scores of 2.2 [2–3] and 2.3 [2–3], respectively), while image distortion was only mild (score of 1.6 [1–2]).

Eleven primary tumours were detected in ten patients (one patient with two analysable primary tumours). All tumours were histologically proven HNSCC of the oro- or hypopharynx. Median volume of the primary tumours was 4.9 [1.1–42.1] ml. Mean PET SUV of the segmented tumours was 5 ± 2.5 (average) and mean ADC values were 1.2 ± 0.3 10^{-3} mm^2/s (average).

Table 2 shows individual values (minimum and mean ADC, maximum and mean PET SUV) of single patients.

In nine of ten patients, we observed a clear negative voxel-wise correlation between ADC and SUV. In voxel-wise correlation, a patient-wise significant negative correlation was observed between ADC values and the corresponding FDG SUV (mean r = –0.31 ± 0.27, $p < 0.05$). Fig. 3 (imaging and scatter plot) shows two imaging examples and the correlating voxel-wise distribution of ADC and PET SUV. The voxel-wise distribution shows an L-shaped form rather than a direct negative correlation.

However, in one patient (patient 6), the correlation coefficient was positive; upon revision of the registration accuracy between PET and DWI, misregistration most likely led to erroneous voxel correlation of a relatively small primary tumour.

Discussion

Purpose of the present study was to investigate the feasibility of multiparametric hybrid PET/MRI of HNSCC in a special radiotherapeutic setup. The use of a special irradiation setup ensuring exact and reproducible patient positioning by

Table 1 Patient, tumour and treatment characteristics

Patient	Age (years)	Gender	PD	Tumour location	TNM classification (8th edition) inclusion criteria: cM0	Therapy
1	52	M	10/2015	A) Oropharynx	A) pT1 pN0 R0	Resection + adj. RCT
				B) Hypopharynx[a]	B) pT2 pN1 R1	
				C) Vallecula[b]	C) pT1 pN1 R1	
2	71	M	12/2015	Hypopharynx	pT1 pN1 (ECE) R1 (CIS)	Resection + adj. RT
3	52	M	02/2016	Oropharynx	pT2 pN2a (ECE) R2	Resection + def. RCT
4	60	M	03/2016	Oropharynx	pT2 pN2c R0	Resection + adj. RCT
5	55	M	04/2016	Oropharynx	pT3 pN2b (ECE) R0	Resection + adj. RCT
6	61	M	04/2016	A) Oropharynx	A) pT1 pN0 R0	Resection + adj. RCT
				B) Uvula[c]	B) pT1 pN3b (ECE) R0	
7	58	M	06/2016	Hypopharynx	pT2 pN2b R0	Resection + adj. RCT
8	66	M	06/2016	Oropharynx	pT3 pN0 R0	Resection + adj. RT
9	61	M	08/2016	Hypopharynx	cT4a cN2c[d]	def. RCT
10	49	M	01/2017	Oropharynx	pT2 pN2 R0	Resection, adj. RT

M male, *PD* primary diagnosis, *ECE* extracapsular extension, *CIS* carcinoma in situ, *adj.* adjuvant, *def.* definitive, *RT* radiotherapy, *RCT* radiochemotherapy

[a]Suspected lesion in CT scan, reevaluated and proofed in re-panendoscopy after study inclusion

[b]Incidental finding during resection, mucosal carcinomatosis, no image correlation

[c]Pathologic proof after inclusion (tumour of 4.5 mm), no image correlation

[d]Reevaluation of tumour extent after PET/MRI: due to oesophageal affection no resection but definitive RCT

Table 2 Individual values: minimum and mean apparent diffusion coefficient (ADC), maximum and mean positron emission tomography (PET) standardized uptake values (SUV) of single patients

	ADCmin (mm^2/s)	ADCmean (mm^2/s)	SUVmax	SUVmean	r
Patient 1	465	1290	7.9	3.6	–0.26
Patient 2	581	1320	4.0	2.5	–0.10
Patient 3	795	1046	3.0	1.6	–0.44
Patient 4	264	981	17.8	8.4	–0.29
Patient 5	679	1654	15.0	7.1	–0.52
Patient 6	626	1338	7.3	4.4	0.34
Patient 7	359	1127	5.3	3.1	–0.46
Patient 8	423	1177	10.3	4.6	–0.52
Patient 9	574	650	17.4	8.7	–0.29
Patient 10	802	1249	13.1	6.1	–0.58

ADC apparent diffusion coefficient, *SUV* standardized uptake value

a thermoplastic mask, flat table and head support, allows for precise image co-registration of the functional information assessed by PET/MRI and the RT planning computed tomography (CT), which is required for precise dose painting and treatment planning.

In our study, by voxel-wise analysis, a significant negative correlation between ADC values and PET SUV could be shown. In all but one patient, the correlation coefficient was negative. Regarding the reevaluation of the registration accuracy in the patient with positive correlation coefficient, a misregistration seems to have caused the erroneous voxel correlation due to a relatively small primary tumour. Small tumours and difficult registration of PET and DWI might therefore be a possible limitation of this kind of investigation.

Though DWI/ADC and PET/SUV aim to analyse different tissue and tumour phenomenon, there might well be a correlation of these parameters, as both cellularity and glucose consumption are assumed to be associated with proliferation of tumour cells and cell viability [16, 17]. However, ambiguous results in several studies not finding a significant correlation of ADC and SUV measurements in HNSCC as well as some histopathological studies favour the theory of complementary but independent biomarkers [18].

Several studies compared sequential imaging results by acquisition of an MRI and an FDG-PET in subsequent settings:

Fruehwald-Pallamar et al. hereby did not find a correlation of FDG uptake and ADC measurements in 31 patients with HNSCC with a time frame of max. 14 days

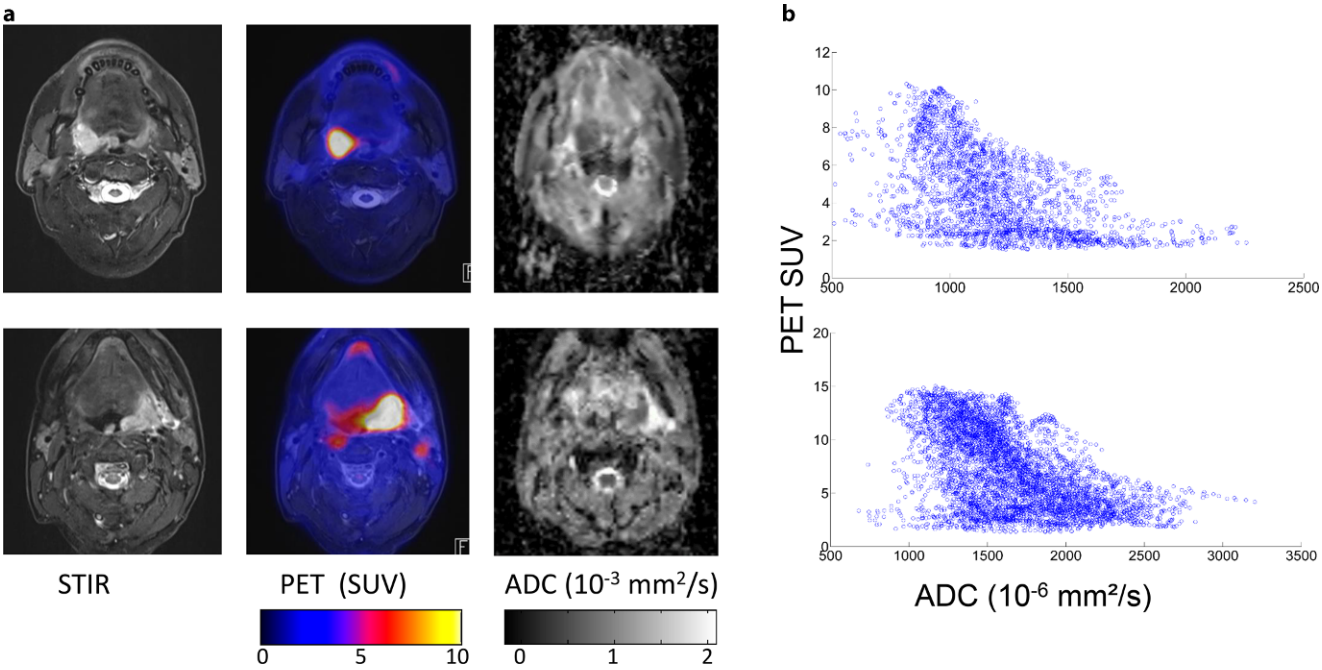

Fig. 3 Examples of acquired imaging data. Two patient examples (top and bottom row) are depicted showing the primary tumour in the morphological sequence (STIR), overlaid with FDG-PET and the ADC map. Corresponding scatterplots showing the L-shaped negative correlation between PET SUV and ADC are shown on the right-hand side. *STIR* short tau inversion recovery sequence, *PET* positron emission tomography, *SUV* standardized uptake value, *ADC* apparent diffusion coefficient

between the examinations [19]. Varoquaux et al. came to the same negative results [16]. A further report of sequential imaging in HNSCC states no correlation between ADC_{1000} or ADC_{2000} and SUVmean, but a positive correlation of the ADC ratio (change of ADC values from b = 1000 to 2000 s/mm²) with SUVmean [20]. Nakajo et al. reported a significant inverse correlation between SUVmax and ADC in HNSCC [21].

Recent studies report on simultaneous investigations by hybrid PET/MRI imaging, due to possible variabilities and uncertainties in subsequent image acquisition settings. Thus, in line with these efforts, our study was conducted in a hybrid setting: advantage of simultaneously obtained data implies reduction of variations in patients' position and avoidance of relevant time-shift between the examinations, which might support more reliable results.

Hereby, Gawlitza et al. found a trend towards negative correlation of ADCmin and SUVmax in 17 patients with primary or recurrent HNSCC receiving PET/MRI [22]. Images distorted by motion artefacts were excluded, indicating that also in hybrid imaging, motion and positioning are relevant issues. By finding this trend toward negative correlation of ADCmin and SUVmax, the authors agree with Nakajo et al. [21] that glycolytic activity might be partly associated with the microstructural environment of HNSCCs.

These results regarding feasibility of image acquisition and potential correlation of glucose metabolism and cellularity are promising to promote precision medicine and in line with our results.

In a subsequent study of this group, eleven patients with HNSCC were investigated prospectively by PET/MRI [18]. In contrast, in this cohort, no significant correlation between SUVmax or SUVmean and various ADC parameters was found. Besides imaging parameters, tumour tissue was analysed pertaining to the tumour proliferation index on Ki67 antigen-stained samples and the nucleic count as well as the total and average nucleic area. ADCmean and ADCmax showed a negative correlation with Ki67 levels, while SUV measurements did not correlate significantly with Ki67 as a marker of the proliferation pathway. However, SUVmax, SUVmean, ADCmean and ADCmax tended to correlate with the average nucleic area. Therefore, the authors postulate that ADC and PET SUV are complementary but independent biological markers in HNSCC.

For further precise analysis, several groups published voxel-based studies, which we used as well to assure accurateness of the data. A recent publication reports on voxel-wise correlation of ADC and SUV measured by PET/MRI, and describes a negative correlation in nine of twelve patients, though emphasizing ambiguous results [23]. Leibfarth et al. also found a negative Pearson correlation of ADC and FDG (r = –0.39) [24].

As far as documented, all studies mentioned above used a conventional diagnostic setup with a head and neck coil. None of the studies described the utilization of a specialised

RT setting or thermoplastic masks for positioning and fixation. The use of our RT setup was chosen to reduce motion artefacts as well as to ensure superior translation into the radiation treatment planning CT and fusion of images for dose painting.

An approach of imaging acquisition for dose painting in radiation position was reported by Houweling et al. in HNSCC [25]: FDG-PET/CT scans were performed in a five-point radiotherapy mask. Images were fused with the planning CT and diagnostic MRIs, including DWI, that were acquired with a neurovascular receive coil within 2 weeks. By voxel-wise correlation of SUV and ADC they found a (low) negative correlation in the majority of tumours, though they describe partly ambiguous information with respect to dose painting targets. Aramburu Núñez et al. investigated six HNSCC patients with sequential MRI and PET/CT, both in radiation setup, and found a significant inverse correlation of pretreatment ADCmean and SUV in five primary tumours and eleven lymph nodes [26]. These findings applying an irradiation setup mostly support our results of a significant negative correlation of ADC values and PET SUV, and encourage our approach of image acquisition.

In our underlying data we observed an L-shaped form of the voxel-wise distribution between ADC and PET SUV rather than a direct negative correlation. This observation has been reported before in HNSCC [24], and also for other tumour entities and localizations, e. g. pulmonary lesions [27]. This distribution may thus represent the underlying tissue composition. A more detailed analysis in larger patient cohorts will be necessary to fully understand its biological significance and diagnostic value.

In conclusion, the relation between DWI and PET SUV imaging still remains controversial. Our data contribute to this issue by showing a significant inverse correlation of ADC and SUV in a voxel-wise analysis and a hybrid setting using a specialised fixation by a thermoplastic mask.

One could hypothesize that by voxel-wise analysis of the data, uncertainties could be reduced. The combination of rigid fixation of the area of interest, hybrid imaging and voxel-wise analysis, reducing movement artefacts and registration issues, supports image quality and might improve the reliability of data. This promising approach might elucidate the ambiguous data of previous studies.

Good diagnostic image quality was achieved and all patients completed the comparatively long protocol (60 min). This might determine a challenging issue, as the RT setup is contraindicated in patients suffering from claustrophobia or with specific pain lying on an RT table overlay for a longer period of time. Shorter protocols might be requested to implement thermoplastic masks in routine diagnostic settings.

Despite the distortion correction technique used in our study, image quality of DWI shows still room for improvement. The implementation of improved shimming techniques such as slice-specific shimming may offer significant progress in this context [28].

The results of voxel-wise analyses are expected to also be influenced by noise leading to uncertainty in quantitative measurements. This factor is, among others, directly influenced by voxel size. It will be of interest to investigate this aspect in future studies, varying acquired image resolution in order to determine optimal trade-offs between resolution and data robustness.

Due to this highly selected cohort in favour of comparability, significant limitations of this study are the comparably small patient and lesion number (ten patients, eleven lesions analysed). Therefore, the data remain preliminary and indicative. Besides, resampling and distortion correction of DWI imaging could imply some uncertainties. Further investigation is required in a bigger cohort of patients to confirm these pilot results.

Conclusion

Multiparametric voxel-wise characterization of HNSCC is feasible using combined PET/MRI in a radiation planning setup. The investigation of DWI and FDG-PET parameters might allow risk stratification, decision support and adaptive radiation treatment planning according to tumour characteristics in future.

Funding We would like to thank the "Zentrum für Personalisierte Medizin (ZPM)" Tübingen/Germany for funding this project. Kerstin Zwirner is supported by the Fortüne/PATE Program of the Medical Faculty, Eberhard Karls University Tübingen (funding number: 2447-0-0).

Compliance with ethical guidelines

Conflict of interest D. Zips has received research grants from Elekta and Siemens. K. Zwirner, D. Thorwarth, R. M. Winter, S. Welz, J. Weiss, N. F. Schwenzer, H. Schmidt, C. la Fougère, K. Nikolaou and S. Gatidis declare that they have no conflict of interest.

Ethical standards All procedures performed in studies involving human participants were in accordance with the ethical standards of the institutional and/or national research committee and with the 1964 Helsinki declaration and its later amendments or comparable ethical standards. This article does not contain any studies with animals performed by any of the authors. Informed consent was obtained from all individual participants included in the study.

References

1. Peeken JC, Nusslin F, Combs SE (2017) "Radio-oncomics": the potential of radiomics in radiation oncology. Strahlenther Onkol 193(10):767–779. https://doi.org/10.1007/s00066-017-1175-0
2. Boss A, Stegger L, Bisdas S, Kolb A, Schwenzer N, Pfister M, Claussen CD, Pichler BJ, Pfannenberg C (2011) Feasibility of si-

multaneous PET/MR imaging in the head and upper neck area. Eur Radiol 21(7):1439–1446. https://doi.org/10.1007/s00330-011-2072-z
3. Wippold FJ 2nd (2007) Head and neck imaging: the role of CT and MRI. J Magn Reson Imaging 25(3):453–465. https://doi.org/10.1002/jmri.20838
4. Combs SE, Nusslin F, Wilkens JJ (2016) Individualized radiotherapy by combining high-end irradiation and magnetic resonance imaging. Strahlenther Onkol 192(4):209–215. https://doi.org/10.1007/s00066-016-0944-5
5. Becker M, Zaidi H (2014) Imaging in head and neck squamous cell carcinoma: the potential role of PET/MRI. Br J Radiol 87(1036):20130677. https://doi.org/10.1259/bjr.20130677
6. Vandecaveye V, De Keyzer F, Dirix P, Lambrecht M, Nuyts S, Hermans R (2010) Applications of diffusion-weighted magnetic resonance imaging in head and neck squamous cell carcinoma. Neuroradiology 52(9):773–784. https://doi.org/10.1007/s00234-010-0743-0
7. Thoeny HC, De Keyzer F, King AD (2012) Diffusion-weighted MR imaging in the head and neck. Radiology 263(1):19–32. https://doi.org/10.1148/radiol.11101821
8. Ng SH, Yen TC, Liao CT, Chang JT, Chan SC, Ko SF, Wang HM, Wong HF (2005) 18 F-FDG PET and CT/MRI in oral cavity squamous cell carcinoma: a prospective study of 124 patients with histologic correlation. J Nucl Med 46(7):1136–1143
9. Baek CH, Chung MK, Son YI, Choi JY, Kim HJ, Yim YJ, Ko YH, Choi J, Cho JK, Jeong HS (2008) Tumor volume assessment by 18 F-FDG PET/CT in patients with oral cavity cancer with dental artifacts on CT or MR images. J Nucl Med 49(9):1422–1428. https://doi.org/10.2967/jnumed.108.051649
10. Al-Ibraheem A, Buck A, Krause BJ, Scheidhauer K, Schwaiger M (2009) Clinical applications of FDG PET and PET/CT in head and neck cancer. J Oncol. https://doi.org/10.1155/2009/208725
11. Gallamini A, Zwarthoed C, Borra A (2014) Positron Emission Tomography (PET) in oncology. Cancers (Basel) 6(4):1821–1889. https://doi.org/10.3390/cancers6041821
12. Werner MK, Schmidt H, Schwenzer NF (2012) MR/PET: a new challenge in hybrid imaging. AJR Am J Roentgenol 199(2):272–277. https://doi.org/10.2214/AJR.12.8724
13. Bhatnagar P, Subesinghe M, Patel C, Prestwich R, Scarsbrook AF (2013) Functional imaging for radiation treatment planning, response assessment, and adaptive therapy in head and neck cancer. Radiographics 33(7):1909–1929. https://doi.org/10.1148/rg.337125163
14. Paulus DH, Thorwath D, Schmidt H, Quick HH (2014) Towards integration of PET/MR hybrid imaging into radiation therapy treatment planning. Med Phys 41(7):72505. https://doi.org/10.1118/1.4881317
15. Winter RM, Schmidt H, Leibfarth S, Zwirner K, Welz S, Schwenzer NF, la Fougere C, Nikolaou K, Gatidis S, Zips D, Thorwarth D (2017) Distortion correction of diffusion-weighted magnetic resonance imaging of the head and neck in radiotherapy position. Acta Oncol 56(11):1659–1663. https://doi.org/10.1080/0284186X.2017.1377347
16. Varoquaux A, Rager O, Lovblad KO, Masterson K, Dulguerov P, Ratib O, Becker CD, Becker M (2013) Functional imaging of head and neck squamous cell carcinoma with diffusion-weighted MRI and FDG PET/CT: quantitative analysis of ADC and SUV. Eur J Nucl Med Mol Imaging 40(6):842–852. https://doi.org/10.1007/s00259-013-2351-9
17. Minn H, Clavo AC, Grenman R, Wahl RL (1995) In vitro comparison of cell proliferation kinetics and uptake of tritiated fluorodeoxyglucose and L-methionine in squamous-cell carcinoma of the head and neck. J Nucl Med 36(2):252–258
18. Surov A, Stumpp P, Meyer HJ, Gawlitza M, Hohn AK, Boehm A, Sabri O, Kahn T, Purz S (2016) Simultaneous (18)F-FDG-PET/MRI: associations between diffusion, glucose metabolism and histopathological parameters in patients with head and neck squamous cell carcinoma. Oral Oncol 58:14–20. https://doi.org/10.1016/j.oraloncology.2016.04.009
19. Fruehwald-Pallamar J, Czerny C, Mayerhoefer ME, Halpern BS, Eder-Czembirek C, Brunner M, Schuetz M, Weber M, Fruehwald L, Herneth AM (2011) Functional imaging in head and neck squamous cell carcinoma: correlation of PET/CT and diffusion-weighted imaging at 3 T. Eur J Nucl Med Mol Imaging 38(6):1009–1019. https://doi.org/10.1007/s00259-010-1718-4
20. Choi SH, Paeng JC, Sohn CH, Pagsisihan JR, Kim YJ, Kim KG, Jang JY, Yun TJ, Kim JH, Han MH, Chang KH (2011) Correlation of 18 F-FDG uptake with apparent diffusion coefficient ratio measured on standard and high b value diffusion MRI in head and neck cancer. J Nucl Med 52(7):1056–1062. https://doi.org/10.2967/jnumed.111.089334
21. Nakajo M, Nakajo M, Kajiya Y, Tani A, Kamiyama T, Yonekura R, Fukukura Y, Matsuzaki T, Nishimoto K, Nomoto M, Koriyama C (2012) FDG PET/CT and diffusion-weighted imaging of head and neck squamous cell carcinoma: comparison of prognostic significance between primary tumor standardized uptake value and apparent diffusion coefficient. Clin Nucl Med 37(5):475–480. https://doi.org/10.1097/RLU.0b013e318248524a
22. Gawlitza M, Purz S, Kubiessa K, Boehm A, Barthel H, Kluge R, Kahn T, Sabri O, Stumpp P (2015) In vivo correlation of glucose metabolism, cell density and microcirculatory parameters in patients with head and neck cancer: initial results using simultaneous PET/MRI. PLoS ONE 10(8):e134749. https://doi.org/10.1371/journal.pone.0134749
23. Rasmussen JH, Norgaard M, Hansen AE, Vogelius IR, Aznar MC, Johannesen HH, Costa J, Engberg AM, Kjaer A, Specht L, Fischer BM (2017) Feasibility of multiparametric imaging with PET/MR in head and neck squamous cell carcinoma. J Nucl Med 58(1):69–74. https://doi.org/10.2967/jnumed.116.180091
24. Leibfarth S, Simoncic U, Monnich D, Welz S, Schmidt H, Schwenzer N, Zips D, Thorwarth D (2016) Analysis of pairwise correlations in multi-parametric PET/MR data for biological tumor characterization and treatment individualization strategies. Eur J Nucl Med Mol Imaging 43(7):1199–1208. https://doi.org/10.1007/s00259-016-3307-7
25. Houweling AC, Wolf AL, Vogel WV, Hamming-Vrieze O, van Vliet-Vroegindeweij C, van de Kamer JB, van der Heide UA (2013) FDG-PET and diffusion-weighted MRI in head-and-neck cancer patients: implications for dose painting. Radiother Oncol 106(2):250–254. https://doi.org/10.1016/j.radonc.2013.01.003
26. Aramburu Nunez D, Lopez Medina A, Mera Iglesias M, Gomez SF, Dave A, Hatzoglou V, Paudyal R, Calzado A, Deasy JO, Shukla-Dave A, Munoz VM (2017) Multimodality functional imaging using DW-MRI and 18 F-FDG-PET/CT during radiation therapy for human papillomavirus negative head and neck squamous cell carcinoma: Meixoeiro Hospital of Vigo Experience. World J Radiol 9(1):17–26. https://doi.org/10.4329/wjr.v9.i1.17
27. Schmidt H, Brendle C, Schraml C, Martirosian P, Bezrukov I, Hetzel J, Muller M, Sauter A, Claussen CD, Pfannenberg C, Schwenzer NF (2013) Correlation of simultaneously acquired diffusion-weighted imaging and 2-deoxy-[18 F] fluoro-2-D-glucose positron emission tomography of pulmonary lesions in a dedicated whole-body magnetic resonance/positron emission tomography system. Invest Radiol 48(5):247–255. https://doi.org/10.1097/RLI.0b013e31828d56a1
28. Gatidis S, Graf H, Weiss J, Stemmer A, Kiefer B, Nikolaou K, Notohamiprodjo M, Martirosian P (2017) Diffusion-weighted echo planar MR imaging of the neck at 3 T using integrated shimming: comparison of MR sequence techniques for reducing artifacts caused by magnetic-field inhomogeneities. MAGMA 30(1):57–63. https://doi.org/10.1007/s10334-016-0582-z